EXPERIMENTAL STUDY ON STATISTICAL CHARACTERISTICS OF PULSE TRANSMISSIONS IN THE SHALLOW WATER

M. Zheng

The University of Birmingham, Edgbaston, Birmingham, B15 2TT, UK
(Formerly from Xiamen University, Xiamen, 361005, China)

1. INTRODUCTION

Underwater acoustic communication is the only effective method to transmit information in the sea and has become increasingly important in recent years. This is mainly attributed to the commercial and military need for acoustic communications in applications such as unmanned-untethered vehicle (UUV) control, offshore-remote operations and oceanographic data telemetering. Three comprehensive bibliographies of past works on underwater acoustic communications are presented in overview articles by Coates & Willison [1], Baggeroer [2] and Catipovic [3].

The Shallow Water Acoustic Channel (SWAC) is much more hostile than any other existing communication channels. It is a bandwidth limited channel with temporal, spatial and frequency-dependent variance, high noise level and severe multipath. The major problems generated by the SWAC can be characterised by statistical fading and Inter-Symbol Interference (ISI) which result from massive multipath propagation.

Statistical characteristics of SWAC behaviour, such as Probability of Density Function (PDF), time correlation function and fluctuation of repetition period, are not theoretically sought because of the extreme complication and variation of SWAC. This is particularly true for high frequency transmission used in communications systems. However, it is just such statistical characteristics that are so essential to the communication engineer.

In this paper, the experimental measurements of statistical characteristics of pulse transmissions in SWAC are presented. The measurements integrate the total effects of the medium inhomogeneities and the boundary reflections. It is shown that the PDFs of the envelope of the mainpath and the multipath of the received pulses are in agreement with a Rician distribution. It is also shown that the coefficient of variation of amplitude of the mainpath is apparently smaller than that of the multipath, and that the correlativity between pulses is high and the fluctuation of repetition period is small. According to the above statistical characteristics, a telemetry system has been developed. It has been proved that the system is robust in the multipath fading SWAC.

2. EXPERIMENT DESIGN AND DATA ANALYSIS

2.1 Experiment Design

The experiments were carried out in Xiamen harbour, Fujian, China, which is 5 nautical miles(nm) long, 3 nm wide, and approximately 16 meters deep at the low tide period. The sea floor in the area is quite flat and made up of clay and coarse sand.

EXPERIMENTAL STUDY ON STATISTICAL CHARACTERISTICS

The experiment took place in September 1986. The velocity profile, a fully developed summer profile typical of that area, was almost isovelocity, sea state was about 3-4. The tonpilz projector was deployed in a fixed location 4 metres under the water, its beamwidth was about 70 degrees at a frequency of 20KHz. An omnidirectional circular hydrophone was buoyed off the bottom as shown in Fig. 1. Tests were performed over ranges of 0.25, 0.5, 1, 2, 3 nm along the length of the harbour. The instrumentation used in the experiment is shown in block diagram form in Fig. 1. A pulsed carrier was generated by a microprocessor (2) controlled gate (3) and a CW constant frequency generator (1). This signal was fed to a power amplifier (4) and a power of about 100W was applied to the transducer (6) via a match transformer (5). The signal was received by a hydrophone (7), and after a pre-amplifier (8) and a wide band amplifier (9), was tape recorded (10). It was also narrow band filtered (11) and monitored on an oscilloscope (12).

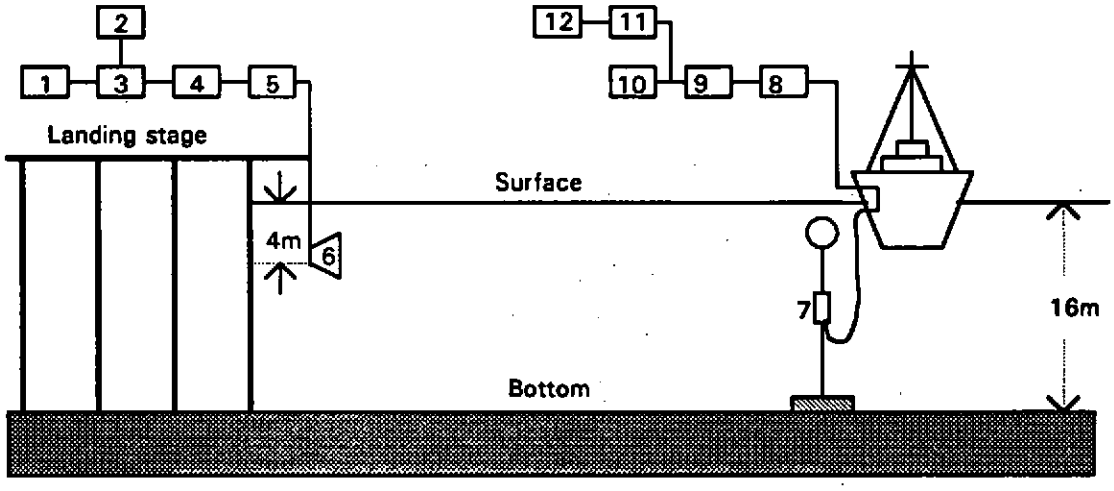

Fig. 1 Experiment layout

An example of typical envelope of received signal is shown in Fig. 2.

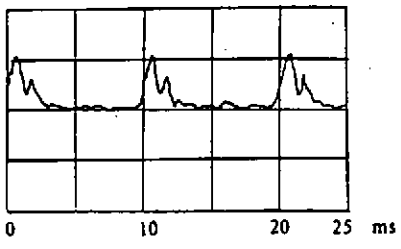

Fig. 2 The envelopes of received signal

2.2 Data Analysis

Data analysis was performed by the data process system based on a HP-85B microcomputer and a HP-3582A spectrum analyser. The HP-85B was used to control the tape recorder, signal capture, and data process.

The received signal is a stochastic process. Processing of stationary or non-stationary stochastic signal is treated separately, it is therefore necessary to test the stationariness of the signal. A non-parameter RUNTEST method was used to test the stationariness of ten groups of mainpath and multipath which lasted 3 minutes. Test results are shown in table 1.

EXPERIMENTAL STUDY ON STATISTICAL CHARACTERISTICS

From table 1 (α=0.05) it can be seen that all data were accepted at 5% level of significance. This means that the received signal is statistically stationary during the 3 minutes analysis time interval, that is, their mean and higher-order statistics, such as variance, do not change during above period. It is reasonable to assume that the received signal has an ergodic property for the real physical stochastic process is usually an ergodic process.

Table 1 The RUNTEST results of mainpath and multipath

Range	Number of samples N	Accepted range $\gamma_{N,\frac{\alpha}{2}}$	Accepted range $\gamma_{N,\frac{\alpha}{2}}$	Mainpath run times γ_1	Multipath run times γ_2
0.25 nm	50	19	32	28	26
0.5 nm	50	19	32	25	25
1 nm	50	19	32	30	26
2 nm	50	19	32	31	30
3 nm	50	19	32	24	25

If the received signal $x(t)$ is stationary and ergodic, then after sampling $x(t)$ becomes the sequence $x(i)$ $(i=1,2,\cdots,N)$. The statistical parameters are as follows.

2.2.1 The one-dimension PDF of amplitude estimation is

$$\hat{p}(x)=\frac{N_y}{NW}$$

where W: the width centring at x

N_y: the times of $x(i)$ falls in $x\pm W/2$

2.2.2 The coefficient of variation of amplitude is

$$\hat{\eta}=\frac{\sigma_0}{a_0}=\frac{\sum_{i=1}^{N}\sqrt{[x(i)-a_0]^2}}{\sum_{i=0}^{N}x(i)}$$

2.2.3 The cross-correlation between j th and k th pulses is

$$\hat{R}_{j,k}=\frac{Cov(X_j,X_k)}{\sqrt{D(X_j)D(X_k)}}=\frac{\frac{1}{M}\sum_{i=1}^{M}x(j)x(k)-\frac{1}{M^2}\sum_{i=1}^{M}x(j)\sum_{i=1}^{M}x(k)}{\sqrt{\{\frac{1}{M}\sum_{i=1}^{M}x^2(j)-[\frac{1}{M}\sum_{i=1}^{M}x(j)]^2\}\{\frac{1}{M}\sum_{i=1}^{M}x^2(k)-[\frac{1}{M}\sum_{i=1}^{M}x(k)]^2\}}}$$

where M is the number of sample points in the received pulse.

2.2.4 The pulse repetition period, the distance between two maximum points of adjacent pulses, is

$$\hat{T}_{k,k+1}=t_{\max}(X_{k+1})-t_{\max}(X_k)$$

if N is sufficiently large, $\hat{p}(x),\hat{\eta},\hat{R}_{j,k}$ and $\hat{T}_{k,k+1}$ tend to be valid statistical descriptions of the stochastic process.

EXPERIMENTAL STUDY ON STATISTICAL CHARACTERISTICS

3. RESULTS AND DISCUSSION

The PDFs of the mainpath and multipath at different ranges are shown in Fig.3. The curves in Fig.3 are a Racian distribution of which the mean value and standard deviation are same as that of the sampled data. Derivation of the parameters a and σ of the Racian distribution is included in Appendix 1. The parameter $\alpha/2$ ($a^2/2\sigma^2$) for the Racian distribution at different ranges is listed in table 2.(note: $\alpha/2$ is signal to noise ratio in the Racian distribution)

Table 2 The parameter $\alpha/2$ of mainpath and multipath

	0.25 nm	0.5 nm	1 nm	2 nm	3 nm
Mainpath	17.3	14.7	12	5	0.7
Multipath	1.4	2.7	3.5	2.3	0

Examination of Fig.3 (a1)-(e1) and (a2)-(e2) shows that the PDFs of the envelopes of the mainpath and multipath are well in agreement with the Racian distribution. Table 2 indicates that the parameter $\alpha/2$ of the mainpath decreases with increasing range. So at short range such as 0.25,0.5,1 nm, PDFs tend to a Gaussian distribution, but at long range, such as 3 nm, the parameter $\alpha/2$,equal to 0.7, is small, therefore PDF becomes a Rayleigh distribution. It is interesting to note that the parameter $\alpha/2$ of multipath increases with increasing range within 1 nm. The explanation is that the grazing angle at short range is relatively large, so the surface influence will be quite strong. Thus the PDF at short range tends to a Rayleigh distribution. However, at long range, since the influence of inhomogeneities, such as microstructure and internal wave, become dominant, the parameter $\alpha/2$ will decrease with increasing range. So the PDF of multipath at long range such as 3 nm tends to a Rayleigh distribution as well.

The correlation between pulses reflects variability of the channel during the observation interval. That is to say, the correlation of mainpath mainly reflects the variation of the refracted index of the body of water; the correlation of multipath reflects the above variation as well as the sea surface variation. From Fig. 4 it can be seen that the correlation of mainpath and multipath are high. Because there is no significant variation of channel during the observation period (40ms). From Fig.3 it also can be seen that the correlation of multipath is weaker than that of mainpath because the multipath includes the variation of the sea surface.

Fig. 5 and 6 show that the coefficient of variation of repetition period of the mainpath and multipath is very small (maximum 8×10^{-3}) and the coefficient of variation of the multipath is larger than that of the mainpath. The reason is similar to the one above, because the coefficient of variation of repetition period is also a reflection of variation of the channel.

The coefficient of variation of amplitude of mainpath with range is shown in Fig 7 and is approximately in agreement with the $r^{1/2}$ relationship that can be predicated by wave theory [4]. However the coefficient of variation of multipath at short range such as 0.25 nm is large, but tends to decrease with increasing range as the grazing angle becomes less. At long range, the influences of inhomogeneities become dominant, so the coefficient of variation of multipath tends to be that of mainpath.

Fig. 8 shows the PDF of amplitude of mainpath added by multipath at the range of 2 nm, there are double peaks in it, the possible explanation is that some low frequency component due to the interference between mainpath and multipath exists in the sampled data or the sampled data is not statistical stationary. Fig. 9 shows that the correlation between pulses of the above signal decreases and the coefficient of variation of repetition period increases compared with mainpath at the same range. This means the signal becomes worse after embedded by multipath.

The correlation between pulses is very strong and the fluctuation of period repetition is very small, one MFSK telemetry system employing such an effect was developed [5]. The signalling structure of this system is shown in Fig. 11 in which frequency f_5 is used to act as a synchronisation pulse and the other four frequencies as coded pulses. Because of low fluctuation of period repetition, the synchronisation pulse can be transmitted after quite long interval. Also because of high correlativity between pulses, the pulse of frequency $f_i\ (i = 1,2,3,4)$ in block 1 can be correlated with the pulses of same frequency in block $n\ (n = 2,3,4)$, which will produce high correlation gain to combat signal fading. In addition, a specific logic was adopted in the receiver to overcome the ISI; each frequency is used only once in one block of coded pulses, once a pulse of frequency $f_i\ (i = 1,2,3,4)$ is received, the receiver will automatically reject the frequency f_i. Theoretical analysis and in situ experiments of the system showed that it is quite robust in a shallow water multipath fading channel, however its bit rate is low.

4. CONCLUSIONS

It has been found that the PDFs of amplitude of mainpath and multipath in the shallow water follows a Racian distribution, at short range, the PDF of mainpath tends to be a Gaussian distribution and multipath tends to be a Rayleigh distribution. At long range, the PDFs of both mainpath and multipath tend to be a Rayleigh distribution. The coefficient of variation of mainpath is apparently smaller than that of multipath. The correlation between pulses is high and fluctuation of repetition period is small. A telemetry system employing the above characteristics has been shown to be robust in the shallow water multipath fading channel.

5. ACKNOWLEDGEMENTS

The author is grateful to Prof. Xu Tianzeng and Associate Prof. Huang Ximing for suggestion and instruction the study of the above subject.

6. REFERENCES

[1] R COATES & P. WILLISON, 'Underwater Acoustic Communications: A Bibliography and Review', *Proc. Inst. Acoustics*, December, , p54,(1987)

[2] A B BAGGEROER, 'Acoustic Telemetry--An Overview' *IEEE J. Oceanic Eng.*, 9, p229, Oct., (1984)

[3] J A CATIPOVIC, "Performance Limitations in Underwater Acoustic Telemetry," *IEEE J. Oceanic Eng.*, 15, p205, (1990)

EXPERIMENTAL STUDY ON STATISTICAL CHARACTERISTICS

[4] G C KNOLLMAN, 'Wave Propagation in a Medium with Random Spheroidal Inhomogeneities', *J. Acoust. Soc. Am.*, 34 p647,(1964)
[5] M ZHENG, T XU & X HUANG, 'MFSK-DTCCA and its Applications to Underwater Acoustic Telemetry', *Int. Conf. Acoust.* 14, p BP-9, (1992)
[6] S O RICE, 'Mathematical Analysis of Random Noise', *Bell Syst. Tech. J.* 24,46,Art 3.10, (1945)
[7] A D WHALEN, *Detection of Signal in Noise*, Academic, New York, (1971)

7. APPENDIX

If A_t is the envelope of the received sinusoidal signal plus additive narrow-band Gaussian noise, its PDF is [6]

$$p(A_t) = \frac{A_t}{\sigma^2}\exp[-\frac{A_t}{2\sigma^2}(A_t^2 + a^2)]I_0(\frac{aA_t}{\sigma^2}) \qquad \text{A-1}$$

where a: Variable amplitude of sinusoidal signal
σ: standard deviation of band-limited noise
$I_0(\frac{aA_t}{\sigma^2})$: Bessel function of the first kind of order zero

From reference [7], we can obtain

$$E(A_t^n) = (2\sigma^2)^{\frac{n}{2}}\Gamma(\frac{n}{2}+1)\,{}_1F_1(-\frac{n}{2},1,-\frac{\alpha^2}{2}) \qquad \text{A-2}$$

where

$$\frac{\alpha}{2} = \frac{a^2}{2\sigma^2}$$

$${}_1F_1(x,y,z) = \frac{\Gamma(y)}{\Gamma(x)}\sum_{n=0}^{\infty}\frac{\Gamma(n+x)}{\Gamma(n+y)}\frac{z^n}{n}$$

$$\Gamma(n) = \int_0^{\infty} t^{n-1}e^{-t}dt \quad t>1$$

From A-2 the mean value and variance (mean square deviation) of a Racian distribution are

$$a_0 = E(A_t) = \sqrt{\frac{\pi}{2}}\sigma_1 F_1(-\frac{1}{2},1,-\frac{\alpha^2}{2}) \qquad \text{A-3}$$

$$\sigma_0^2 = D(A_t) = E(A_t^2) - [E(A_t)]^2 = 2\sigma^2(1-\frac{\alpha^2}{2}) - a_0 \qquad \text{A-4}$$

From equation A-3 and A-4 it is difficult to get analytic solution for the parameters σ and α, but it is easy to obtain numeric solution. Thus the latter method was used to obtain the parameters σ and α.

EXPERIMENTAL STUDY ON STATISTICAL CHARACTERISTICS

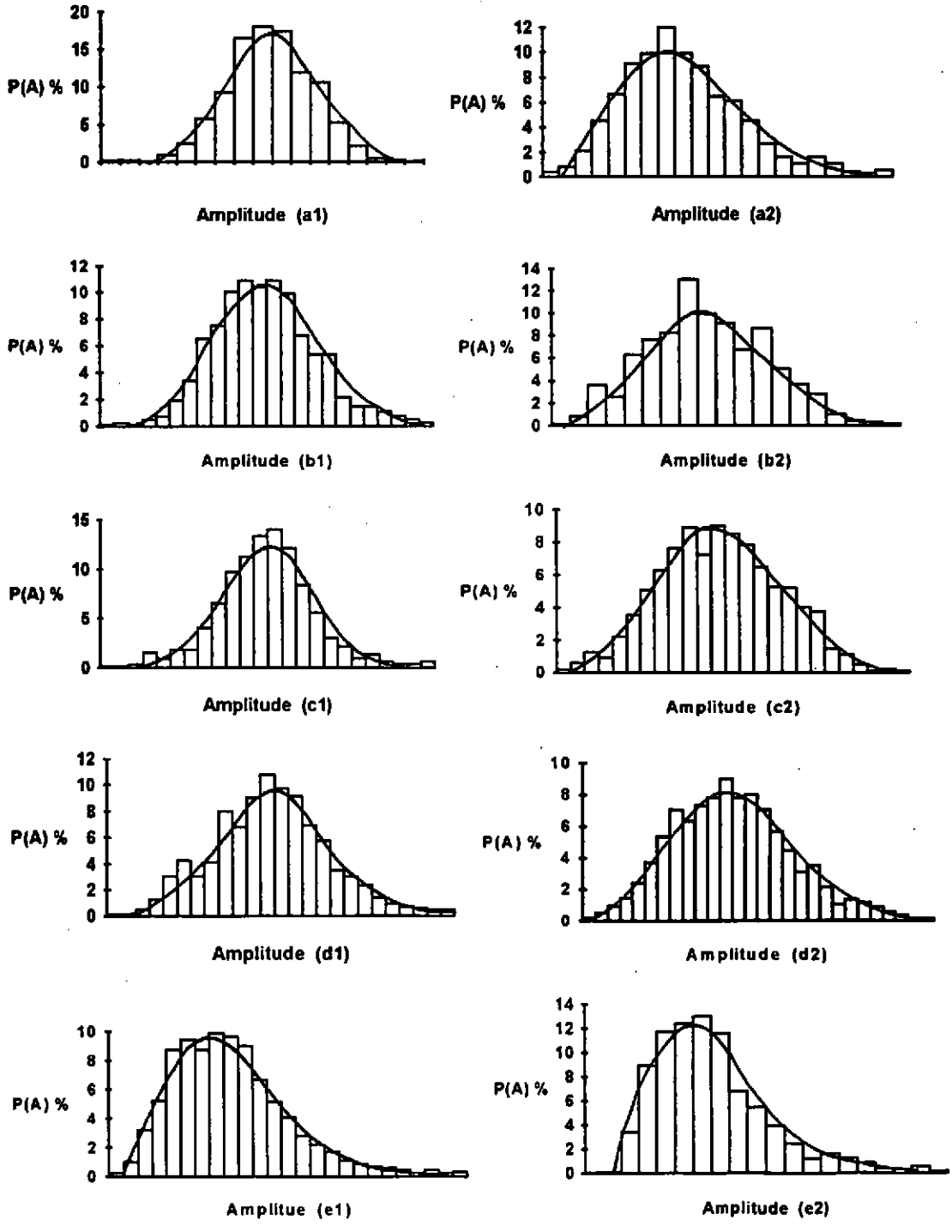

Fig. 3 The PDF of mainpath and multipath
(a): 0.25 nm, (b):0.5 nm, (c):1nm, (d): 2 nm, (e): 3 nm.
Number 1 denotes mainpath and number 2 denotes multipath

EXPERIMENTAL STUDY ON STATISTICAL CHARACTERISTICS

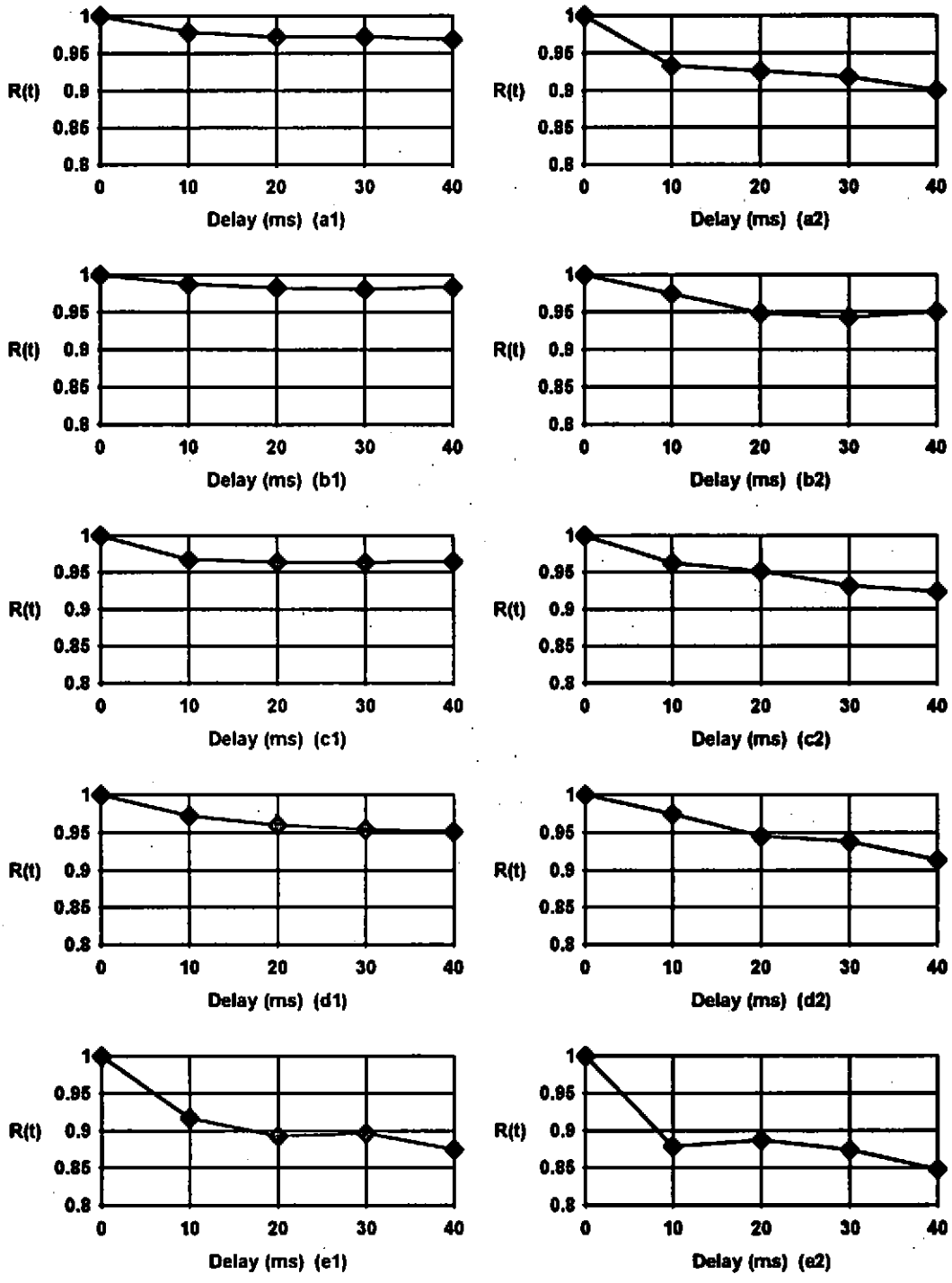

Fig. 4 The correlation between pulses
(a): 0.25 nm, (b):0.5 nm, (c):1nm, (d): 2 nm, (e): 3 nm.
Number 1 denotes mainpath and number 2 denotes multipath

EXPERIMENTAL STUDY ON STATISTICAL CHARACTERISTICS

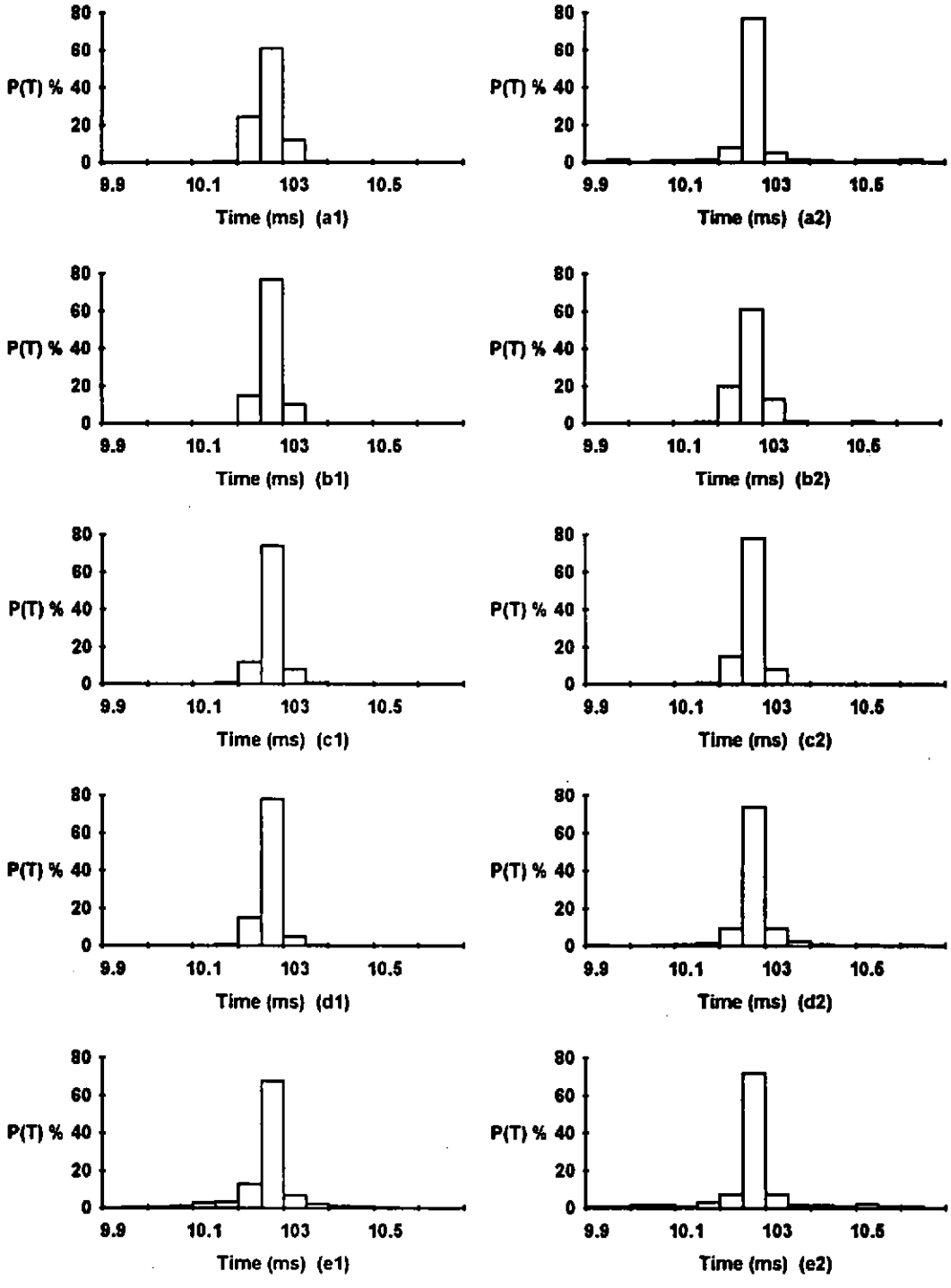

Fig. 5 The PDF of repetition period
(a): 0.25 nm, (b):0.5 nm, (c):1nm, (d): 2 nm, (e): 3 nm.
Number 1 denotes mainpath and number 2 denotes multipath

EXPERIMENTAL STUDY ON STATISTICAL CHARACTERISTICS

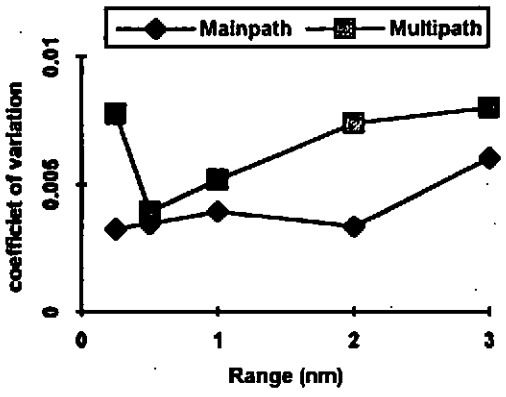

Fig. 6 Coefficient of variation of repetition period

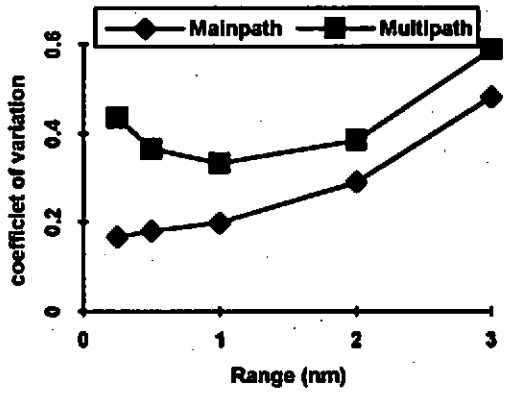

Fig. 7 Coefficient of variation of amplitude

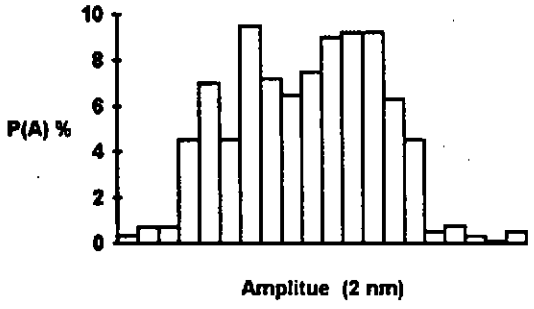

Fig. 8 The PDF of envelope of mainpath embedded by multipath

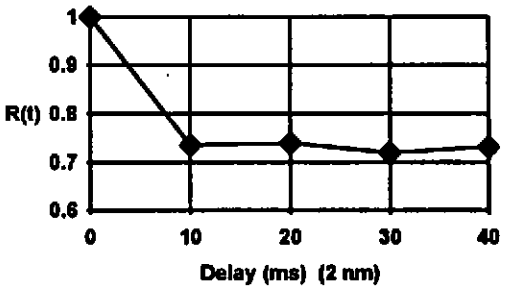

Fig. 9 The correlation between pulses of mainpath embedded by multipath

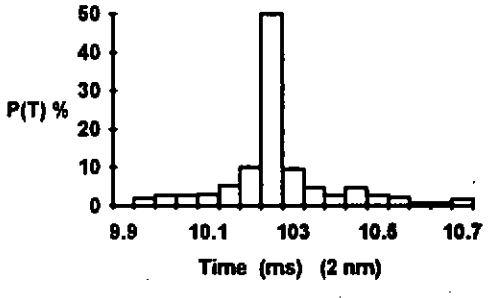

Fig.10 The PDF of repetition period of mainpath embedded by multipath

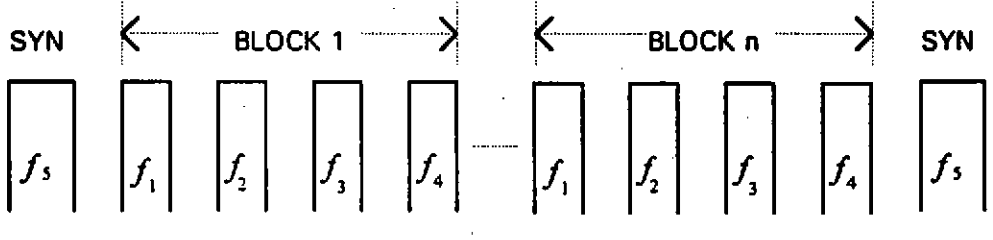

Fig. 11 Signalling structure of the MFSK telemetry system